OPTICAL REVIEW Vol. 17, No. 3 (2010) 223–229

Monte Carlo Simulation of Spectral Reflectance Using a Multilayered Skin Tissue Model

Takaaki MAEDA, Naomi ARAKAWA[1], Motoji TAKAHASHI[1], and Yoshihisa AIZU

Division of Science for Composite Functions, Muroran Institute of Technology, 27-1 Mizumoto, Muroran, Hokkaido 050-8585, Japan
[1]*Shiseido Research Center, 2-2-1 Hayabuchi, Tsuzuki, Yokohama 224-8558, Japan*

(Received August 31, 2009; Accepted December 12, 2009)

A nine-layered skin tissue model is newly developed for the Monte Carlo simulation of spectral reflectance. The derivation of the necessary parameters for each of the nine layers in the simulation is presented, in which the parameters used in the conventional three-layered model are modified on the basis of some histological findings on skin and reported examples. Using appropriate optical and geometrical parameters, simulated spectra can be produced that agree well with measured spectra. This approach provides a flexible means of spectral fitting to measured results and of estimating changes in the parameters of skin tissue.

Keywords: skin tissue, spectral reflectance, Monte Carlo simulation, scattering coefficient, absorption coefficient, spectral fitting

1. Introduction

Optics plays an important role in diagnostics and therapeutics in dermatology and in skin care treatments in cosmetics. When light enters skin tissue, it propagates while being absorbed by chromophores such as melanin and hemoglobin and being scattered by cells, fibers, and tissue. In general, the penetration depth of light in the visible wavelength range into skin tissue is considered to be about 1–3 mm.[1)] This is roughly in agreement with the thickness of skin tissue from the stratum corneum to the epidermis, dermis, and subcutaneous layers treated in dermatology. Any physiological or structural change in these tissue layers, which may be caused by various skin diseases or disorders, thus affects the propagation of light through absorption and scattering. This is usually a wavelength-dependent phenomenon and can be experimentally observed through the spectral reflectance of skin. Dermatological phenomena are often recognized by changes in skin color and doctors are familiar with the relation between skin diseases and skin color. As is well known, skin color and spectral reflectance can be directly related to each other by spectrocolorimetry. In these respects, spectral reflectance is very useful information for quantitative color and physiological analyses of skin tissue.[2)]

Analyzing the elemental factors of absorption and scattering from skin spectral reflectance is a type of inverse problem. Solving the problem is generally difficult because skin tissue has a complicated structure and physiology, and thus various factors may affect the reflectance. Some methods have been developed to treat this problem using modeling approaches. The theoretical modeling of light propagation in tissue-like random media, which was studied on the basis of the diffusion approximation to the Boltzmann transport equation,[3–5)] gives analytic solutions in some limited cases. In contrast, stochastic numerical modeling using a Monte Carlo (MC) simulation[6,7)] is advantageous since it has greater freedom and is applicable in general cases. A main drawback with MC simulation is its long computation time, but this is not fundamental problem owing to advances in computing. A number of MC algorithms have been used to study light transport in tissue media[6–15)] over the last two decades. Among them, the algorithm[12)] based on a layered-tissue model is extensively known and used for various applications including the simulation of light propagation in skin tissue. In the MC simulation of skin spectral reflectance, a two- or three-layered tissue model, which consists of the epidermis, dermis, and subcutaneous tissue, is generally used since it is convenient and easy to compute. However, this model is unsatisfactory for applications to various skin diseases and disorders. For example, skin pigmentation results in a change in chromophore concentration in a specifically localized region within the epidermis or dermis. However, the two- or three-layered model assumes a homogeneous distribution of chromophores over the epidermis or dermis and thus cannot treat chromophore localization. Meglinski and Matcher[16,17)] developed a seven-layered model and reported the simulation of skin spectral reflectance. However, their algorithm assumes a wavelength-independent scattering coefficient and anisotropy scattering parameter, and also fiber-optic measurement geometry, and is thus still unsatisfactory for the realistic simulation of skin spectral reflectance.

In this paper, we propose the use of a nine-layered skin tissue model, which was developed on the basis of histological features of human skin tissue. To execute on MC simulation using this model, it is required to specify all the values of the necessary parameters, i.e., the scattering coefficient, absorption coefficient, anisotropy scattering parameter, refractive index, and thickness in each of the nine layers. We found a suitable combination of these values by considering skin histological characteristics with the numbers of layers increased from three to nine. Results demonstrated good agreement between measured and simulated spectral reflectance curves.

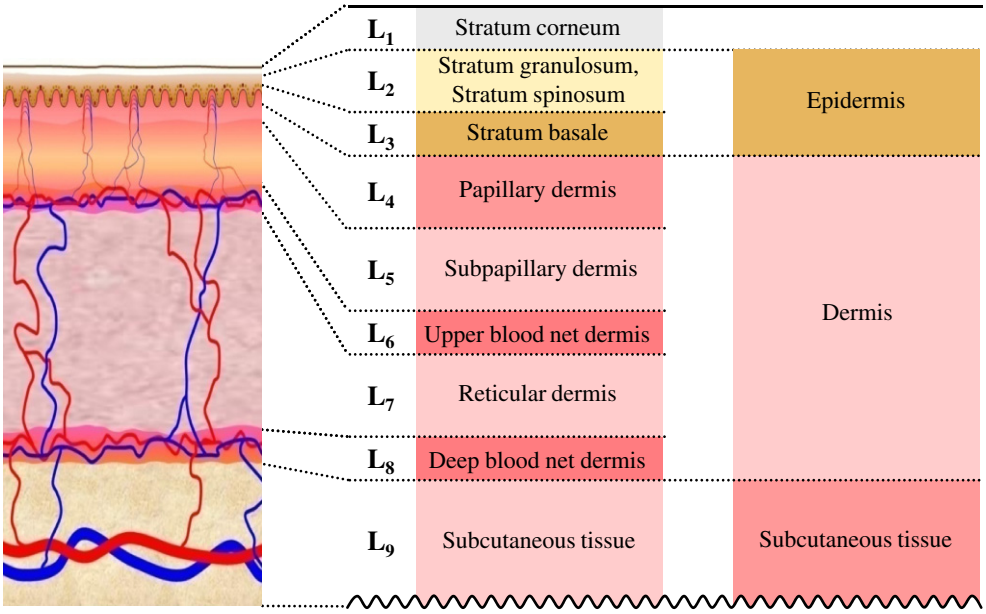

Fig. 1. (Color online) Schematic structures of (a) skin tissue, (b) nine-layered model, and (c) three-layered model.

2. Skin Tissue and Multilayered Model

It is known that human skin is organized into different types of tissues and vessels with a complex structure. Figure 1 shows a schematic structure of skin tissue. The skin tissue is roughly divided into three main layers, the epidermis, dermis, and subcutaneous fat layer, which correspond to the three-layered model shown in Fig. 1(c). From the histological viewpoint, however, it should be treated in more detail. The stratum corneum (L_1) of about 10 µm thickness comprises the top surface of skin, and the epidermis exists under layer L_1. The epidermal layer is composed of the stratum granulosum and stratum spinosum (L_2), and the stratum basale (L_3). The thickness of the epidermis is usually about 100 µm or less. The dermis is under the epidermis and is classified into five layers consisting of the papillary dermis (L_4), subpapillary dermis (L_5), upper blood net dermis (L_6), reticular dermis (L_7), and deep blood net dermis (L_8). The dermis has a total thickness of about 1.5 mm. The subcutaneous tissue (L_9) is approximately 5–10 mm in thickness and is under the dermis.

The skin has grooves in the top surface called the sulcus cutis. There is a characteristic boundary consisting of an epidermal rete ridge and dermal papilla or the epidermal-dermal interface (between L_3 and L_4). This capillary extends from the arteriole and venule in the subcutaneous tissue into the dermis and forms a reticulation type of blood vessel layer (L_8) in the lower part of the dermis and a vascular network (L_6) in the upper part of the dermis. Part of the capillary also reaches the dermal papilla in the epidermis/dermis layer interface (between L_3 and L_4). Moreover, a large number of fiber components such as collagen and elastin exist in the dermis and maintain the elasticity of the skin. It is known that both of these are related to scattering properties in the tissue.[1)] On the other hand, pigments such as carotene in the granulosa layer (the upper part of layer L_2), melanin in the epidermis (mainly the basal layer L_3), and hemoglobin in the dermis are related to optical absorption properties, which depend on their concentration.

In previous conventional simulations, we employed a two- or three-layered skin tissue model, and the stratum corneum (L_1) and subcutaneous tissue (L_9) were omitted.[18–21)] However, the epidermal and dermal layers have a laminar structure with two or more sublayers as shown in Fig. 1(a). In the dermis, the vasculature is not homogeneous and the oxygen saturation of hemoglobin must be distributed inhomogeneously. The volume and composition of fibrillary elements might also vary. Therefore, it cannot be assumed that absorption and scattering are uniform over the epidermis and dermis. Detailed and appropriate modeling thus cannot be achieved in the conventional simulation. Thus, we newly developed a nine-layered model based on the structural features of the multilayers in skin tissue as shown in Figs. 1(a) and 1(b). The proposed model is expected to enable the more realistic MC simulation of skin spectral reflectance than the two- or three-layered model. By setting various values for optical and geometrical parameters in each of the nine layers, one can simulate various spectral reflectances under different conditions.

3. Monte Carlo Simulation

In the MC simulation of light transport in tissue media, light is treated as a bundle of photons. Random numbers generated by a computer statistically determine the trajectories of photons in the media, which are characterized by optical properties such as absorption coefficient μ_a and scattering coefficient μ_s. Figure 2 shows a conceptual diagram of the MC method. A photon bundle of unit energy

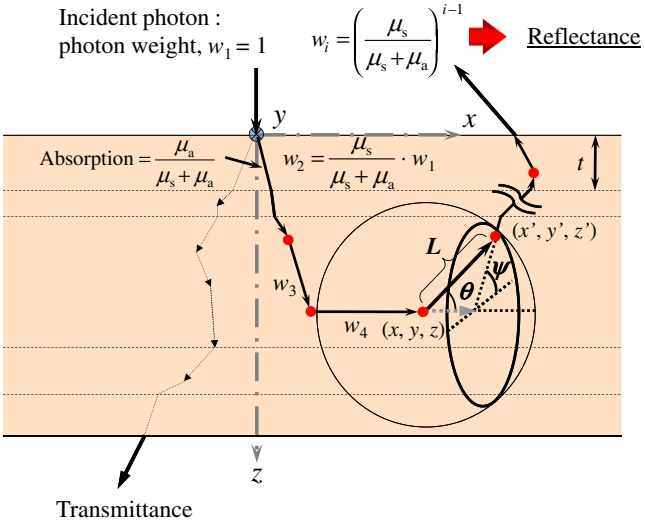

Fig. 2. (Color online) Schematic diagram of Monte Carlo simulation of light propagation in multilayered model.

enters the tissue and undergoes scattering and absorption. As the photon travels a distance L, the probability that it undergoes neither an absorbing event nor a scattering event is given by $\exp[-(\mu_s + \mu_a)L]$. Then, the free path length L_f is derived as $\ln r_1/(\mu_s + \mu_a)$, where r_1 is a random number ranging from 0 to 1. After traveling a distance L_f, the photon energy is assumed to be attenuated at a rate of $\mu_s/(\mu_s + \mu_a)$. If the resultant energy is smaller than a preset threshold, then this photon bundle is regarded as negligibly attenuated, and the second photon bundle enters the tissue. When the energy is still larger than the threshold, propagation continues and the new traveling direction (θ, ψ) of the photon bundle is given by $\theta = f^{-1}(r_2), \psi = 2\pi r_3$,

$$f(\theta) = \frac{1}{2}\int_0^{\theta} p(\theta')\sin\theta'\, d\theta', \qquad (1)$$

where r_2 and r_3 are random numbers between 0 and 1. $p(\theta)$ is the phase function and gives the scattered light intensity distribution with respect to the deflection angle θ, and $f(\theta)$ is the cumulative angle distribution function of $p(\theta)$. The azimuthal angle is given by ψ. By accumulating the energies of photons that are emitted from the top surface to the detection side, reflectance is calculated with reference to the total energy of incident photons. This process is performed at each of the necessary wavelengths, and thus spectral reflectance can be obtained numerically.

In this study, the above process is performed in the wavelength range of 380–780 nm at intervals of 10 nm. To obtain stable simulation results, 10^5–10^7 photons are usually necessary from our experience. For the MC simulation here, we used the algorithm of Wang *et al.*,[12] in which five input parameters must be specified at a given wavelength λ for each layer: scattering coefficient $\mu_s(\lambda)$, absorption coefficient $\mu_a(\lambda)$, anisotropy scattering parameter $g(\lambda)$, refractive index $n(\lambda)$, and thickness t. $g(\lambda)$ is the average cosine value of the phase function, and it ranges from -1 to $+1$, corresponding to perfect backscattering and forward scattering. The algorithm by Wang *et al.* employs the Henyey-Greenstein function[22] as a well-known approximated form of the phase function. As given in Table 1, typical values of $g(\lambda)$ are 0.7–0.8 for tissue and greater than 0.9 for blood, which indicate that skin tissue typically has a strong forward-scattering property. The refractive index n is a wavelength-dependent function but here is assumed to be constant in the wavelength range used. Errors due to this assumption are generally negligible in the visible spectral range.

Table 1. Optical parameters and thicknesses for the seven-layered model of Meglinski and Matcher.[16,17]

No.	Name of layer	μ_a (mm^{-1})	μ_s (mm^{-1})	g	n	t (mm)
1	Stratum corneum	0.00586	100	0.86	1.50	0.02
2	Living epidermis	0.00482	45	0.80	1.34	0.08–0.1
3	Papillary dermis	0.03341	30	0.90	1.40	0.15–0.2
4	Upper blood net dermis	0.24130	35	0.95	1.39	0.08–0.1
5	Reticular dermis	0.03341	25	0.80	1.40	1.4–1.6
6	Deep blood net dermis	0.08078	30	0.95	1.38	0.08–0.12
7	Subcutaneous fat	0.04127	5	0.75	1.44	6.0–6.5

$\lambda = 633$ nm

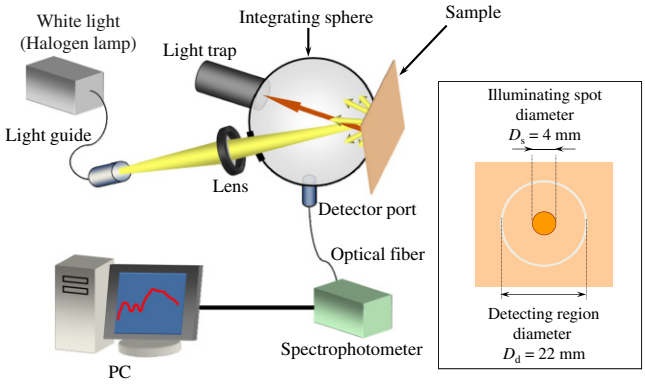

Fig. 3. (Color online) Experimental setup for spectral reflectance measurements.

4. Results and Discussion

4.1 Results obtained with three-layered model

We first measured the diffuse reflectance spectra of skin tissue in the wavelength range of 380–780 nm as sample data for comparison purposes. Figure 3 illustrates the experimental setup for measuring diffuse reflectance spectra. Light from a halogen lamp source (Hayashi LA-150UX) without a cold mirror, which covers the visible to near-IR wavelength range, was focused via a light guide and lens to a spot diameter of 4 mm onto the surface of skin tissue. The diameter and focal length of the lens were 54 and 100 mm, respectively. Diffusely reflected light from the tissue, which was placed at the sample port of an integrating sphere (Labsphere RT-060-SF) was received at the input face of a fiber probe having 400 μm diameter connected to the detector port. The detected area of the skin was circular with a diameter of 22 mm. The fiber transmitted the received light

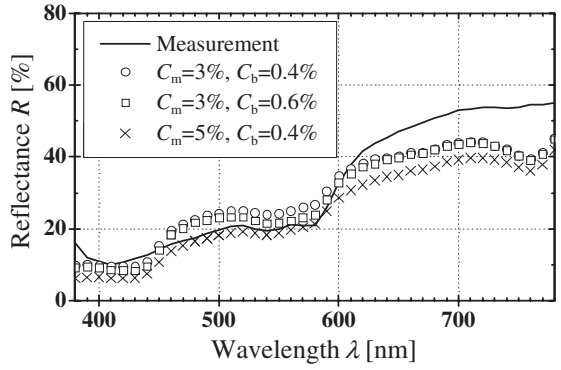

Fig. 4. Simulated results obtained with the three-layered model and measured result.

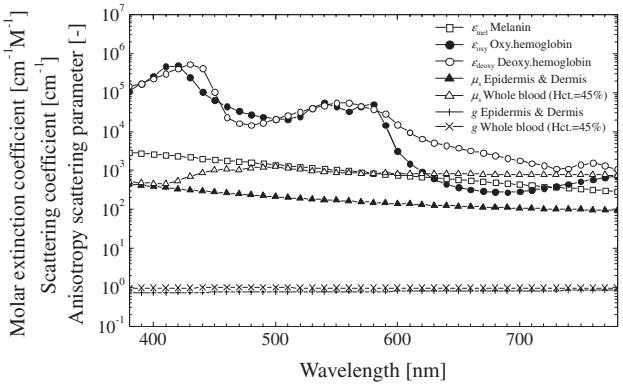

Fig. 5. Optical parameters used for the MC simulation.

into a multichannel spectrophotometer (Ocean Optics SD-2000), which measures reflectance spectra in the visible to near-IR wavelength range under the control of a personal computer (PC).

Figure 4 shows the measured result for the sampled and the simulated results obtained with the previously used three-layered model. Here, C_m and C_b are melanin and hemoglobin concentrations, which are related to the absorption coefficients $\mu_{a,e}(\lambda)$ and $\mu_{a,d}(\lambda)$ in the epidermis and dermis by $\mu_{a,e}(\lambda) = C_m\varepsilon_{mel}(\lambda)$ and $\mu_{a,d}(\lambda) = C_b\varepsilon_{hb}(\lambda)$, respectively. $\varepsilon_{mel}(\lambda)$ and $\varepsilon_{hb}(\lambda)$ are the extinction coefficients of melanin and total hemoglobin, respectively, and the latter is expressed by

$$\varepsilon_{hb}(\lambda) = SaO_2 \cdot \varepsilon_{oxy}(\lambda) + (1 - SaO_2) \cdot \varepsilon_{deoxy}, \qquad (2)$$

where SaO_2 denotes the oxygen saturation of hemoglobin. The spectra of these coefficients are known and are shown in Fig. 5.[18] The oxygen saturation was set to be 70%, and the hematocrit of blood was assumed to be 45%. Thus, the absorption coefficients μ_a were set to be 18, 0.35, and 0.43 cm^{-1} for the epidermis, dermis, and subcutaneous tissue, respectively, at a wavelength of 633 nm as an example. The scattering coefficient $\mu_s(\lambda)$ and anisotropy parameter $g(\lambda)$ were cited from published values for the epidermis and dermis as shown in Fig. 5. The refractive index n was assumed to be 1.4 for all three layers. The thickness values t were 0.66, 1.94, and 6.0 mm for the epidermis, dermis, and subcutaneous tissue, respectively. The number of photons used was 10^5 and the preset threshold was 10^{-3} in the present MC simulation. The computation time generally depends on the scattering and absorption coefficient values, and was roughly 20 min for one spectrum with 41 wavelength points between 380 and 780 nm with a 10 nm interval using a 3.1 GHz Athlon 64 X2 CPU. An example of a measured spectrum was obtained from the upper arm of a 27-year-old Japanese male. The simulated spectra were found to be significantly low in the long-wavelength range compared with the measured spectrum. We attempted to adjust each of the parameters in the three layers to reduce errors in this range by fitting to the measured spectrum, but errors increased at other wavelengths.

4.2 Parameters for nine-layered model

We first employed the values of the parameters shown in Table 1, which were used in the work of Meglinski and Matcher,[16,17] to perform a MC simulation of skin spectral reflectance with the nine-layered model. In their work, seven layers were used to model the skin structure, while our present model contains nine layers. The stratum granulosum/stratum spinosum (L_2) and stratum basale (L_3) in our model correspond to the "living epidermal layer" in their model, and the papillary dermis (L_4) and subpapillary dermis (L_5) in our model correspond to their single papillary dermis. In accordance with this correspondence, we extended their data to those for the nine-layered model, including the use of a wavelength-independent scattering coefficient μ_s and anisotropy scattering parameter g. This simulation produced a rather strange spectral curve that had much worse agreement with measured results than the curves in Fig. 4 obtained with the three-layered model. One of the reasons for this failure is probably due to the use of a wavelength-independent scattering coefficient and anisotropy scattering parameter and inappropriate values of the absorption coefficient. Next, we attempted to extend the values of the parameters shown in Fig. 5 used for our conventional three-layered model to those applicable to the nine-layered model by modifying them referring to the values of Meglinski and Matcher. The spectra of the parameters in Fig. 5 are derived from typical values cited in the literature.[6,23–34] The absorption coefficient is given by the product of the molar extinction coefficient and the given concentration C_m or C_b of melanin or hemoglobin, respectively.

To extend the previous parameter values to those for the nine-layered model, we employed the first approximation for parameters presented by Jacques[23] because the parameters for the three-layered model were designed using the same principles as those in the approximation. The absorption coefficient in the stratum corneum (L_1) is based on a baseline amount of skin absorption excluding the effects of melanin and hemoglobin, and is given by

$$\mu_{a,sb}(\lambda) = 0.244 + 85.3\exp\left(-\frac{\lambda\ [\mathrm{nm}] - 154}{66.2}\right)\quad (\mathrm{cm}^{-1}). \qquad (3)$$

In the epidermis, i.e., the stratum granulosum/stratum spinosum (L_2) and stratum basale (L_3), the absorption coefficient is a weighted sum of the minor baseline skin absorption and the dominant melanin absorption, and is given by

$$\mu_{a,e}(\lambda) = C_m \mu_{a,m}(\lambda) + (1 - C_m)\mu_{a,sb}(\lambda) \quad (cm^{-1}), \quad (4)$$

where C_m is the melanin concentration or volume fraction occupied by melanosomes, and typical values are $C_m =$ 1.3–6.3% for light-skinned adults, 11–16% for moderately pigmented adults, and 18–43% for darkly pigmented adults. In experience of our laboratory, $C_m = 8$–16% is a useful example for typical Japanese. Melanin is a polymer formed by the condensation of tyrosine molecules and is found in the melanosomes of 1–2-μm-diameter membranous particles. The average absorption coefficient of a melanosome, $\mu_{a,m}$, is approximated by[26]

$$\mu_{a,m}(\lambda) = (6.6 \times 10^{11}) \cdot \lambda\ [nm]^{-3.33} \quad (cm^{-1}). \quad (5)$$

There are two different types of melanin, eumelanin and pheomelanin, and these should be distinguished if necessary. For a conventional MC simulation, the above equation can be used as the first approximation regardless of the melanin type. According to the histology of normal skin, the melanin content is higher in the stratum basale (L_3) than in the stratum granulosum/stratum spinosum (L_2). We set a factor k_{mel} as

$$[\mu_{a,e}(\lambda) \text{ for } L_2] = k_{mel} \cdot [\mu_{a,e}(\lambda) \text{ for } L_3]. \quad (6)$$

An appropriate value of k_{mel} may be chosen experimentally through the optimization of results.

The absorption coefficient in the dermis is determined by the dominant hemoglobin absorption, and is given by

$$\mu_{a,d}(\lambda) = C_b \mu_{a,b}(\lambda) \quad (cm^{-1}), \quad (7)$$

where C_b is the hemoglobin concentration or volume fraction of blood in the dermis. The absorption coefficient of whole blood, $\mu_{a,b}(\lambda)$, is calculated by

$$\mu_{a,b}(\lambda) = 2.303 \times \frac{G}{W} \times \varepsilon_{hb}(\lambda) \quad (cm^{-1}), \quad (8)$$

where $\varepsilon_{hb}(\lambda)$ [l/(mol·cm)] is the molar extinction coefficient of hemoglobin[28] shown in Fig. 5, and is a variable depending on the oxygen saturation SaO_2 as expressed by eq. (2). In accordance with the curve reported by Meglinski and Matcher,[17] we take $SaO_2 = 80\%$ as a normal condition. The hemoglobin concentration in blood of 45% hematocrit G (g/l) and the gram molecular weight of hemoglobin W (g/mol) are typically 150 and 64,500, respectively. The blood is inhomogeneously distributed in the dermis and, thus, the absorption coefficient takes different values among the six layers L_4–L_9. From the histological viewpoint, the upper blood net dermis (L_6) and deep blood net dermis (L_8) are likely to be richer in blood than the other layers. Thus, $\mu_{a,d}(\lambda)$ in eq. (7) cannot be used for the nine-layered model. We employed a proportion of the absorption coefficient values among the six layers given by Meglinski and Matcher[17] to the weight $\mu_{a,b}(\lambda)$ for each of the layers L_4–L_9. Then, we set a weighting factor k_b instead of C_b as

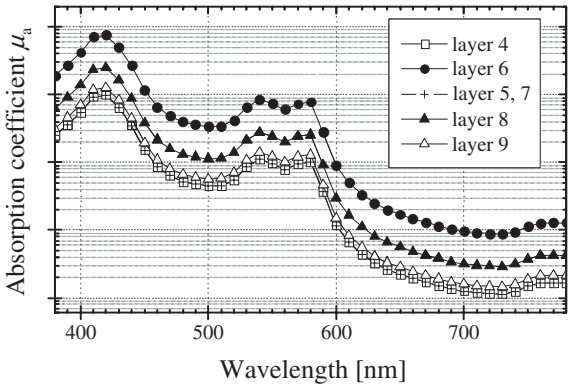

Fig. 6. Spectra of absorption coefficients μ_a in layers L_4–L_9.

$$[\mu_a(\lambda) \text{ for each layer}] = k_b \cdot \mu_{a,b}(\lambda). \quad (9)$$

From various trial MC simulation samples, we use values of k_b in the range 0.01–0.5 depending on each layer condition. Figure 6 shows an example of the resultant absorption coefficient spectra, in which the spectra for L_4, L_5, and L_7 take the same value.

The scattering coefficient of the epidermis and dermis can be approximated as a standard value by using the relation given by Jacques[23] as

$$\mu_{s,s}(\lambda) = \frac{\mu'_{s,R}(\lambda) + \mu'_{s,M}(\lambda)}{1 - g}, \quad (10)$$

where $\mu'_{s,R}(\lambda)$ and $\mu'_{s,M}(\lambda)$ are the contributions due to Rayleigh scattering by the small-scale structure and due to Mie scattering by collagen fibers in skin tissue, respectively, and are given by

$$\mu'_{s,R}(\lambda) = (2 \times 10^{12})\lambda\ [nm]^{-4} \quad (cm^{-1}), \quad (11)$$

$$\mu'_{s,M}(\lambda) = (2 \times 10^{15})\lambda\ [nm]^{-1.5} \quad (cm^{-1}). \quad (12)$$

As far as we know, there is no data available for the weighting $\mu_{s,s}(\lambda)$ for each of the eight layers L_1–L_8. To specify the absorption coefficient $\mu_s(\lambda)$ for each layer, we set a factor k_s as

$$[\mu_s(\lambda) \text{ for each layer}] = k_s \cdot \mu_{s,s}(\lambda). \quad (13)$$

From a number of results obtained by MC simulation, use values of k_s in the range 0.1–10 depending on each layer structure. Appropriate values may be converged to small range through the optimization of results. For the subcutaneous tissue layer (L_9), the scattering coefficient is approximated in our laboratory, in accordance with some discrete values reported by Simpson *et al.*,[35] as

$$\mu_s(\lambda) = k_{s9} \times 527 \exp\left(-\frac{\lambda\ [nm]}{222}\right) + 99 \quad (cm^{-1}), \quad (14)$$

where k_{s9} is again obtained empirically.

The anisotropy parameter of the epidermis and dermis is approximately given as a standard value by van Gemert *et al.*,[36]

$$g(\lambda) = 0.62 + 0.29 \times 10^{-3} \times \lambda \text{ [nm]}. \quad (15)$$

However, this parameter takes a value higher than 0.9 for a bloody tissue layer. To specify this parameter for each layer, we employed a proportion of the g-values among seven layers given by Meglinski and Matcher[17] to the weight $g_s(\lambda)$ for each of the nine layers L_1–L_9. Thus, although our g-values at 633 nm are the same as their values,[17] ours are wavelength-dependent.

We assumed that the refractive index is wavelength-independent in the visible wavelength range. There is in fact a slight dependence on wavelength but it is negligible in usual cases. On this assumption, we employed the refractive index values for the seven layers given by Meglinski and Matcher.[17] The thickness of each of the nine layers generally takes a range of values. It is also different between lightly exposed skin and non-exposed skin. As the first approximation, the data in Table 1[17] are typical and reasonable and are thus used in the present study.

4.3 Results obtained with nine-layered model

Figure 7 shows simulated results obtained with the nine-layered model, which were adjusted so that they fit with the measured spectrum. The measured spectral samples were obtained on the upper arm of (a) a 27-year-old male, (b) a 51-year-old male, and (c) a 24-year-old female. The measured spectrum in Fig. 7(a) is the same as that in Fig. 4. The simulated spectra for the three cases are found to agree well with the measured spectrum. Moreover, the fitting result was clearly improved by using the nine-layered model, in comparison with the results of using the three-layered model in Fig. 4. This improvement is probably due to the adjustability of parameters in the epidermis and dermis by introducing the nine-layered model. We also derived the color difference ΔE between the simulation and measurement, which was evaluated in the CIELAB color space with a D_{65} light source and a 2° view as the observation condition. We confirmed that ΔE was (a) 4.93, (b) 1.99, and (c) 0.59 for the results in Fig. 7. It is generally considered[37] that one cannot perceive the difference between two colors for the case of $\Delta E < 1$–3. Thus, the values in Figs. 7(a)–7(c) are reasonable and provide evidence of good fitting performance. It was also found that the present simulation can be used to model skin regardless of gender and age.

A difficulty in the present MC simulation is adjusting the parameter values appropriately for the nine layers. At present, this adjustment is based on experience. Of course, typical skin spectral reflectance can be simulated with parameters to obtain a first approximation, as presented in this study. However, reliable spectral fitting requires the optimization of parameter values and their combination. A neural network or genetic algorithm may be applied for this purpose,[32,38] but the solution may include unexpected errors due to local minima. To address this subject, we should further investigate the relations between spectral behavior and the change in each parameter from a histological viewpoint.

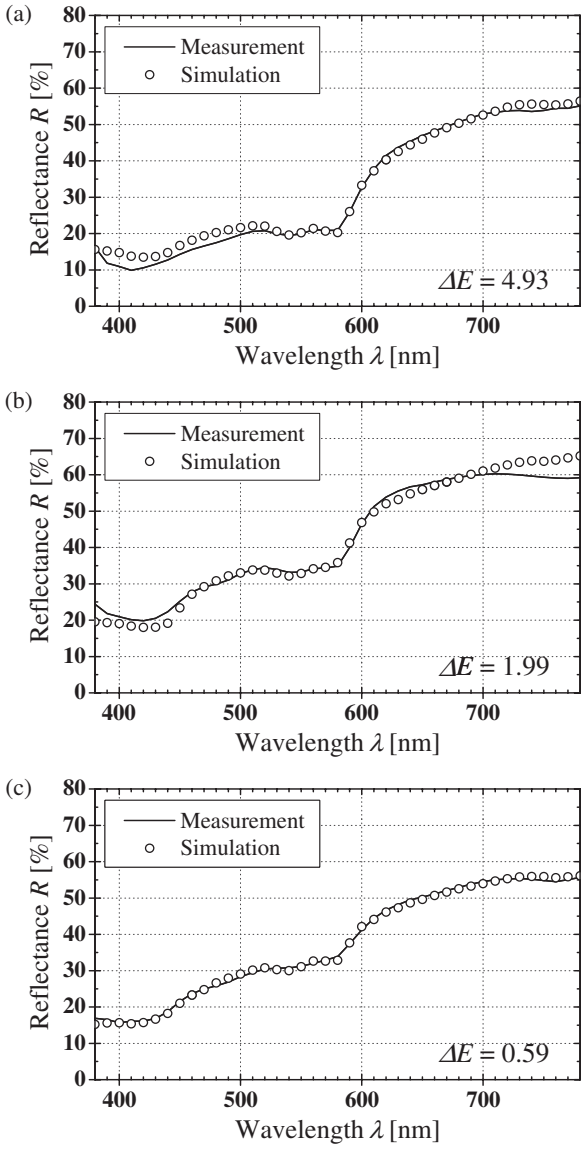

Fig. 7. Simulated results obtained with the nine-layered model and measured results: (a) 27-year-old male, (b) 51-year-old male, and (c) 24-year-old female.

5. Conclusions

We developed a multilayered skin tissue model and performed an MC simulation of skin spectral reflectance by specifying the necessary parameters. The nine-layered skin tissue model was newly introduced on the basis of histological findings on skin tissue, and various combinations of optical parameters for all the layers were considered. The simulated results present a good approximation to the measured results. It is also possible to employ more than nine layers using the framework outlined in this study. This approach provides a useful tool for the estimation and analysis of the spectral reflectance, color, and optical properties related to the skin physiology. However, in parameter setting it is important that one considers the actual skin tissue structure and physiological characteristics. We intend to confirm the applicability of this approach for various skin conditions in the near future.

References

1) V. Tuchin: *Tissue Optics: Light Scattering Methods and Instruments for Medical Diagnosis* (SPIE Press, Bellingham, WA, 2000) Chap. 1, p. 3.
2) A. A. Stratonnikov and V. B. Loschenov: J. Biomed. Opt. **6** (2001) 457.
3) A. Ishimaru: *Wave Propagation and Scattering in Random Media* (Academic, New York, 1978).
4) T. J. Farrell, M. S. Patterson, and B. Wilson: Med. Phys. **19** (1992) 879.
5) A. Kienle and M. S. Patterson: J. Opt. Soc. Am. A **14** (1997) 246.
6) B. C. Wilson and G. Adam: Med. Phys. **10** (1983) 824.
7) R. F. Bonner, R. Nossal, S. Havlin, and G. H. Weiss: J. Opt. Soc. Am. A **4** (1987) 423.
8) M. Keijzer, S. L. Jacques, S. A. Prahl, and A. J. Welch: Laser Surg. Med. **9** (1989) 148.
9) S. T. Flock, M. S. Patterson, B. C. Wilson, and D. R. Wyman: IEEE Trans. Biomed. Eng. **36** (1989) 1162.
10) S. A. Prahl, M. Keijzer, S. L. Jacques, and A. J. Welch: SPIE Inst. Ser. **5** (1989) 102.
11) I. V. Yaroslavsky and V. V. Tuchin: Opt. Spectrosc. **72** (1992) 934.
12) L. Wang, S. L. Jacques, and L. Q. Zheng: Comput. Methods Programs Biomed. **47** (1995) 131.
13) E. Okada, M. Firbank, M. Schweiger, S. R. Arridge, M. Cope, and D. T. Delpy: Appl. Opt. **36** (1997) 21.
14) I. V. Meglinsky and S. J. Matcher: Med. Biol. Eng. Comput. **39** (2001) 44.
15) I. V. Meglinski and S. J. Matcher: Opt. Spectrosc. **91** (2001) 654.
16) I. V. Meglinski and S. J. Matcher: Physiol. Meas. **23** (2002) 741.
17) I. V. Meglinski and S. J. Matcher: Comput. Methods Programs Biomed. **70** (2003) 179.
18) I. Nishidate, Y. Aizu, and H. Mishina: Opt. Rev. **10** (2003) 427.
19) I. Nishidate, Y. Aizu, and H. Mishina: J. Biomed. Opt. **9** (2004) 700.
20) I. Nishidate, Y. Aizu, and H. Mishina: Opt. Lett. **30** (2005) 2128.
21) I. Nishidate, T. Maeda, Y. Aizu, and K. Niizeki: J. Biomed. Opt. **12** (2007) 054006.
22) L. G. Henyey and J. L. Greenstein: Astrophys. J. **93** (1941) 70.
23) S. L. Jacques: http://omlc.ogi.edu/news/jan98/skinoptics.html (1998).
24) A. Roggan, M. Friebel, K. Dorschel, A. Hahn, and G. Muller: J. Biomed. Opt. **4** (1999) 36.
25) W.-F. Cheong, S. A. Prahl, and A. J. Welch: IEEE J. Quantum Electron. **26** (1990) 2166.
26) S. L. Jacques and D. J. McAuliffe: Photochem. Photobiol. **53** (1991) 769.
27) S. L. Jacques, R. D. Glickman, and J. A. Schwartz: Proc. SPIE **2681** (1996) 468.
28) S. A. Prahl: http://omlc.ogi.edu/spectra/hemoglobin/summary.html (1999).
29) P. Agache and P. Humbert: *Measuring the Skin* (Springer, Heidelberg, 2004).
30) T. Dai, B. M. Pikkula, L. V. Wang, and B. Anvari: Phys. Med. Biol. **49** (2004) 4861.
31) D. Y. Churmakov, I. V. Meglinski, and D. A. Greenhalgh: J. Biomed. Opt. **9** (2004) 339.
32) R. Zhang, W. Verkruysse, B. Choi, J. A. Viator, B. Jung, L. O. Svaasand, G. Aguilar, and J. S. Nelson: J. Biomed. Opt. **10** (2005) 024030.
33) T. Gambichler, R. Matip, G. Moussa, P. Altmeyer, and K. Hoffmann: J. Dermatol. Sci. **44** (2006) 145.
34) R. R. Anderson and S. A. Parrish: J. Invest. Dermatol. **77** (1981) 13.
35) R. Simpson, J. Laufer, M. Kohl, M. Essenpreis, and M. Cope: Proc. SPIE **2979** (1997) 307.
36) M. J. C. van Gemert, S. L. Jacques, H. J. C. M. Sterenborg, and W. M. Star: IEEE Trans. Biomed. Eng. **36** (1989) 1146.
37) R. W. G. Hunt: *Measuring Color* (Fountain, London, 1998).
38) W. Verkruysse, R. Zhang, B. Choi, G. Lucassen, L. O. Svaasand, and J. S. Nelson: Phys. Med. Biol. **50** (2005) 57.